Development of Nonpolar Surfaces in the Folding of *Escherichia coli* Dihydrofolate Reductase Detected by 1-Anilinonaphthalene-8-sulfonate Binding†

Bryan E. Jones,‡ Patricia A. Jennings,§ Richard A. Pierre, and C. Robert Matthews*

Department of Chemistry, Biotechnology Institute, and Center for Biomolecular Structure and Function, The Pennsylvania State University, University Park, Pennsylvania 16802

Received June 2, 1994; Revised Manuscript Received August 30, 1994⊗

ABSTRACT: The development of nonpolar surfaces during the folding of *Escherichia coli* dihydrofolate reductase (DHFR) was studied by monitoring the time-dependent fluorescence of 1-anilinonaphthalene-8-sulfonate (ANS) included in the refolding solution. Stopped-flow refolding experiments demonstrated a rapid increase in fluorescence intensity within the dead time of mixing (5 ms), indicating that the earliest detectable folding intermediate contains hydrophobic surfaces which are capable of binding ANS. A further increase in fluorescence intensity over the next 300 ms coincides with the formation of a set of four intermediates which are known to contain a specific tertiary contact [Kuwajima, K., Garvey, E. P., Finn, B. E., Matthews, C. R., & Sugai, S. (1991) *Biochemistry 30,* 7693−7703]. Experiments performed in the presence of polar fluorescence quenching agents indicate that the binding sites for ANS in the burst phase species are more exposed to solvent than those in the subsequent set of intermediates. When considered along with the above study of the formation of secondary structure by stopped-flow circular dichroism, these results imply that DHFR initially forms a molten globule intermediate. Subdomains containing specific tertiary structure and more solvent-excluded ANS binding sites then form before ultimately being converted to native or native-like conformations during the rate-limiting steps in the folding of DHFR. The occurrence of similar kinetic phases observed by ANS binding during the folding of a number of other proteins suggests that this may be a common scheme for protein folding reactions.

The hydrophobic effect has long been thought to provide an important contribution to the stability of globular proteins (Kauzmann, 1959). The free energy gained by removing nonpolar side chains from the aqueous solvent and sequestering them within the interior of the folded protein is proposed to be the principal driving force in overcoming the entropy penalty incurred by organizing a random coil polypeptide into a single native conformation (Kim & Baldwin, 1990; Dill, 1990). The contributions of hydrogen bonding and ionic interactions, although thought to play lesser roles in stability, have recently gained renewed attention on the basis of mutational studies (Shirley *et al.*, 1992; Perry *et al.*, 1989; Dao-pin *et al.*, 1991; Chen *et al.*, 1992; Loewenthal *et al.*, 1992; Serrano *et al.*, 1992). The small magnitude of the free energy of folding of most globular proteins 5−15 kcal/mol (Pace, 1975), implies that all three types of noncovalent interactions will prove to be important in defining the stability of globular proteins.

Given the significance of the hydrophobic effect, hydrogen bonding, and ionic interactions in determining the fully folded, native conformations, it is pertinent to inquire as to their roles during the folding reactions which yield functional proteins. Stopped-flow circular dichroism (CD;[1] Kuwajima, 1989, and references within) and quench-flow hydrogen exchange NMR (Jennings & Wright, 1993; Briggs & Roder, 1992; Udgaonkar & Baldwin, 1990) studies on the folding of a growing number of proteins provide information on the development of secondary structure and stable hydrogen-bonding networks. Mutational analyses offer valuable insights into the contributions of individual side chains to the formation of tertiary structure during folding (Garvey *et al.*, 1989; Goldenberg *et al.*, 1989; Matouschek *et al.*, 1989; Matouschek *et al.*, 1992). Because nonpolar side chains are often involved in clusters, it would be very useful to obtain complementary information on the development of such clusters which ultimately evolve into the tightly packed hydrophobic interior characteristic of the native form.

Ptitsyn and his colleagues (Semisotnov *et al.*, 1991; Ptitsyn *et al.*, 1990) have applied a fluorescent dye binding technique, first developed to characterize hydrophobic surfaces on folded proteins (Stryer, 1965), to examine such surfaces on folding intermediates. The folding of α-lactalbumin and carbonic anhydrase in the presence of ANS is accompanied by a significant increase in ANS fluorescence intensity within the dead time of mixing, less than 20 ms (Semisotnov *et al.*, 1991). In both cases, the fluorescence intensities continued to increase for 100−200 ms before decreasing to the levels displayed by the binding of the dye to the native conformations. An increase in ANS fluorescence intensity in the 100-ms time range followed by a subsequent decrease has also been observed for several other

† This work was supported by NSF Grant MCB 9317273 to C.R.M.

* Author to whom correspondence should be addressed.

‡ Present address: Department of Biochemistry, University of Washington, Seattle, WA 98195.

§ Present address: Department of Chemistry, University of California, San Diego, La Jolla, CA 92093.

⊗ Abstract published in *Advance ACS Abstracts,* October 15, 1994.

[1] Abbreviations: ANS, 1-anilinonaphthalene-8-sulfonate; CD, circular dichroism; DHFR, dihydrofolate reductase from *Escherichia coli*; K_2EDTA, ethylenediaminetetraacetic acid dipotassium salt; MTX, methotrexate; $NADP^+$, nicotinamide adenine dinucleotide phosphate, oxidized form; NMR, nuclear magnetic resonance spectroscopy; UV, ultraviolet.

0006-2960/94/0433-15250$04.50/0

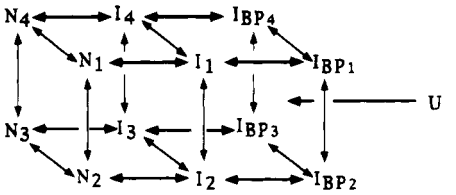

FIGURE 1: Proposed kinetic folding mechanism of DHFR from *E. coli* taken from Jennings *et al.* (1993), modified to incorporate four separate burst phase intermediates (I_{BP_i}).

proteins (Ptitsyn *et al.*, 1990). Although the burst phase reaction (i.e., that occurring within the dead time of mixing) was not examined, inspection of the data in Figure 3 of Ptitsyn *et al.* (1990) suggests that ANS is bound in this phase as well. Taken together, these results demonstrate that ANS can monitor two types of reactions which may reflect common developments in the formation of nonpolar surfaces during the folding of these proteins.

It has been suggested that the initial, burst phase reaction corresponds to the formation of a premolten globule species, a conformation characterized by weakly associated secondary structural elements and a loosely packed hydrophobic core (Chaffotte *et al.*, 1992; Semisotnov *et al.*, 1991). The subsequent increase in ANS intensity has been attributed to the appearance of the molten globule itself (Ptitsyn *et al.*, 1990), a species which is more compact and contains substantial secondary structure but no specific tertiary structure (Kuwajima, 1989; Ptitsyn, 1987). Dihydrofolate reductase from *Escherichia coli* offers an opportunity to test these interpretations.

DHFR is an α/β-sheet protein which has been proposed to fold through a series of intermediates in four parallel channels (Jennings *et al.*, 1993; Figure 1). The first partially folded forms, $I_{BP_1}-I_{BP_4}$, appear within 5 ms and have approximately 40% of the far-UV CD signal observed for the native conformation (Kuwajima *et al.*, 1991). These species (I_{BP_i}) have marginal stability relative to the unfolded form and offer no evidence for specific tertiary structure. Over the next 200 ms a set of four intermediates (I_1-I_4) in which Trp47 and Trp74 attain a native-like packing appear (Kuwajima *et al.*, 1991). These intermediates then fold through four parallel, rate-limiting steps to a corresponding set of native conformers which ultimately relax to the equilibrium distribution (Jennings *et al.*, 1993).

The changes in the fluorescence intensity of ANS during the folding of DHFR were found to follow the same pattern as was observed for carbonic anhydrase and α-lactalbumin (Semisotnov *et al.*, 1991). Following a significant increase in ANS fluorescence intensity in the burst phase (<5 ms), the fluorescence intensity further increases as the dye becomes bound to folding intermediates which contain specific tertiary structure. Refolding of DHFR in the presence of both ANS and polar fluorescence quenching agents demonstrated that the dye bound to the set of burst phase intermediates is relatively exposed to solvent. Diminished quenching of the subsequent phase implies that the dye is then sequestered in a nonpolar region(s) which may exist at the interface of folded but not yet properly docked subdomains. Similar developments of nonpolar surfaces may occur for other proteins.

EXPERIMENTAL PROCEDURES

Reagents. Ultrapure urea was purchased from ICN Biomedicals (Costa Mesa, CA) and used without further purification. High-purity ANS was purchased from Molecular Probes (Eugene, OR). Ultrapure cesium chloride was purchased from Bethesda Research Laboratories (Gaithersburg, MD). All other chemicals were of reagent grade or better. All experiments were performed using a 10 mM potassium phosphate buffer (pH 7.80) containing 0.2 mM K_2EDTA and 1 mM β-mercaptoethanol at 15 °C.

Protein Purification. DHFR was obtained from *E. coli* strain AG-1 (Stratagene) containing the plasmid pWT1-3. This plasmid contains the wild-type DHFR gene whose expression is controlled by an engineered Shine–Delgarno sequence and a consensus promoter (M. Iwakura, personal communication). DHFR was purified as previously described (Jennings *et al.*, 1993). Protein concentration was determined spectroscopically using an extinction coefficient of 3.11×10^4 M^{-1} cm^{-1} at 280 nm (Touchette *et al.*, 1986). The purity of the protein was >95% on the basis of the observation of a single band on Coomassie blue-stained sodium dodecyl sulfate and native polyacrylamide gels (Laemmli, 1977). The specific activity of purified protein measured according to the method of Hillcoat *et al.*, 1967) was found to range from 75 units mg^{-1} to 100 units mg^{-1}; the reported activity of wild-type DHFR is 85 units mg^{-1} under these conditions.

Spectroscopic Methods. All folding experiments were performed on a Bio-Logic SFM-3 stopped-flow spectrometer. ANS fluorescence, measured as photomultiplier tube voltage, was obtained by excitation at 370 nm with a 10-mm slit width and observation of the emission at wavelengths greater than 460 nm with a ground glass filter from Durrum. The cuvette path length was 2.0 mm and the dead time was 5 ms as measured by monitoring the oxidation of tryptophan by *N*-bromosuccinimide (Peterman, 1979). The concentration of ANS was determined using an extinction coefficient of 6.8×10^3 M^{-1} cm^{-1} at 370 nm in methanol (provided by Molecular Probes). Refolding experiments in the presence of ANS typically contained 200 μM ANS and 20 μM DHFR; the measured relaxation times did not depend on either protein or ANS concentration (data not shown). ANS fluorescence experiments in the presence of the quenchers cesium chloride or potassium iodide were done using the same conditions as above, except that the total salt concentration was maintained at 0.5 M by the addition of KCl.

Steady-state fluorescence emission spectra were taken on a Spex Fluorolog spectrometer. The path length was 1 cm, and excitation was at 370 nm with a slit width of 0.3 mm. Emission was recorded from 450 to 600 nm. Intensities in the presence of quenchers were recorded as integrations of the total intensity from 460 to 600 nm using the software provided by Spex.

The binding of the inhibitor, MTX, to DHFR during folding was monitored by changes in absorbance at 380 nm on the Bio-Logic spectrometer (Jennings *et al.*, 1993). The path length of the cuvette was 1 cm, and the slit width was 1 mm. The dead time for the Bio-Logic spectrometer in this configuration was 4 ms when measured using the reduction of 2,6-dichlorophenolindophenol by ascorbic acid (Tonomura *et al.*, 1978). The MTX concentration was determined using an extinction coefficient of 2.21×10^4 M^{-1} cm^{-1} at 302 nm in 0.1 M NaOH (Stone *et al.*, 1984). The final concentrations of MTX and DHFR were 50 and 45 μM, respectively.

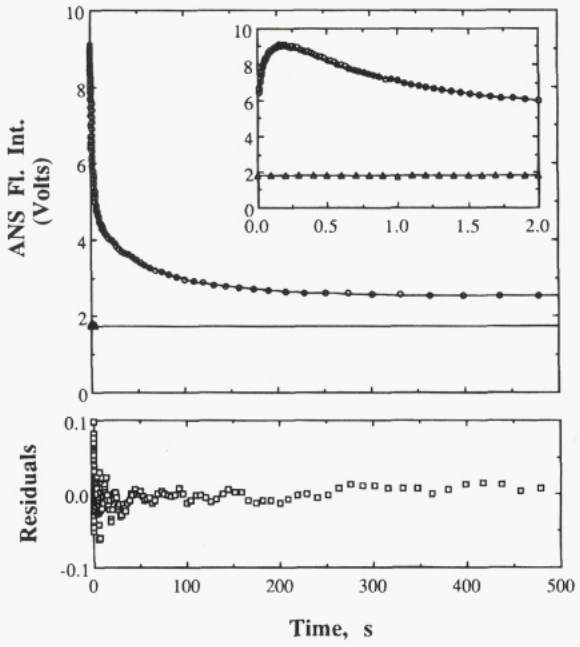

FIGURE 2: Representative kinetic trace obtained during the refolding of DHFR (20 μM) in the presence of ANS (200 μM). The solid line is the fit of the data to a sum of five exponentials; the inset shows the first 2 s of the reaction. Free ANS intensity is indicated by open triangles. The residuals for a nonlinear least squares fit to a sum of five exponentials are shown in the lower panel. The refolding jump was initiated by dilution of a solution of DHFR in 5.4 M urea with buffer containing ANS to a final urea concentration of 0.6 M; the buffer contained 10 mM potassium phosphate, 0.2 mM K_2EDTA, and 1 mM β-mercaptoethanol; the temperature was maintained at 15 °C.

Data Fitting. All kinetic data were fit to a sum of exponentials as previously described (Touchette *et al.*, 1986), using NLIN (SAS Institutes, Cary, NC) running on an IBM RS 6000 workstation.

RESULTS

The fluorescence intensity of ANS during the folding of DHFR is sensitive to all of the transient events previously detected for the folding of this protein. Within 5 ms, there was a dramatic increase in emission intensity, as measured by photomultiplier voltage, from 1.8 to 6.2 V (Figure 2, inset). This burst phase reaction was followed by a further increase to 9.0 V in the 300-ms time range before a slow, multiexponential decrease to the value observed for native DHFR, 2.6 V. The enhanced fluorescence of ANS bound to the native conformation of DHFR was determined to reflect binding to the substrate, i.e., dihydrofolate, site by competition with MTX, a tight-binding competitive inhibitor (data not shown). This binding pocket is in a nonpolar cleft between the two structural domains in DHFR (Figure 3), a site which might be expected to enhance ANS fluorescence.

The data following the burst phase could be fit to the sum of five exponentials, whose relaxation times and relative amplitudes are shown in Table 1. The relaxation time of the phase during which the fluorescence increases to a maximum, τ_5, is 250 $\pm$ 3 ms. This phase is followed by four slower phases, τ_1–τ_4, whose relaxation times range from 1.65 to 125 s. The accuracy of this fit is demonstrated by the random distribution of residuals shown in the bottom panel of Figure 2.

The use of an external probe such as ANS to monitor protein folding reactions raises the possibility that the binding of the probe to the protein may perturb the folding reaction. This possibility was examined by comparing the observed relaxation times to those obtained from intrinsic probes and

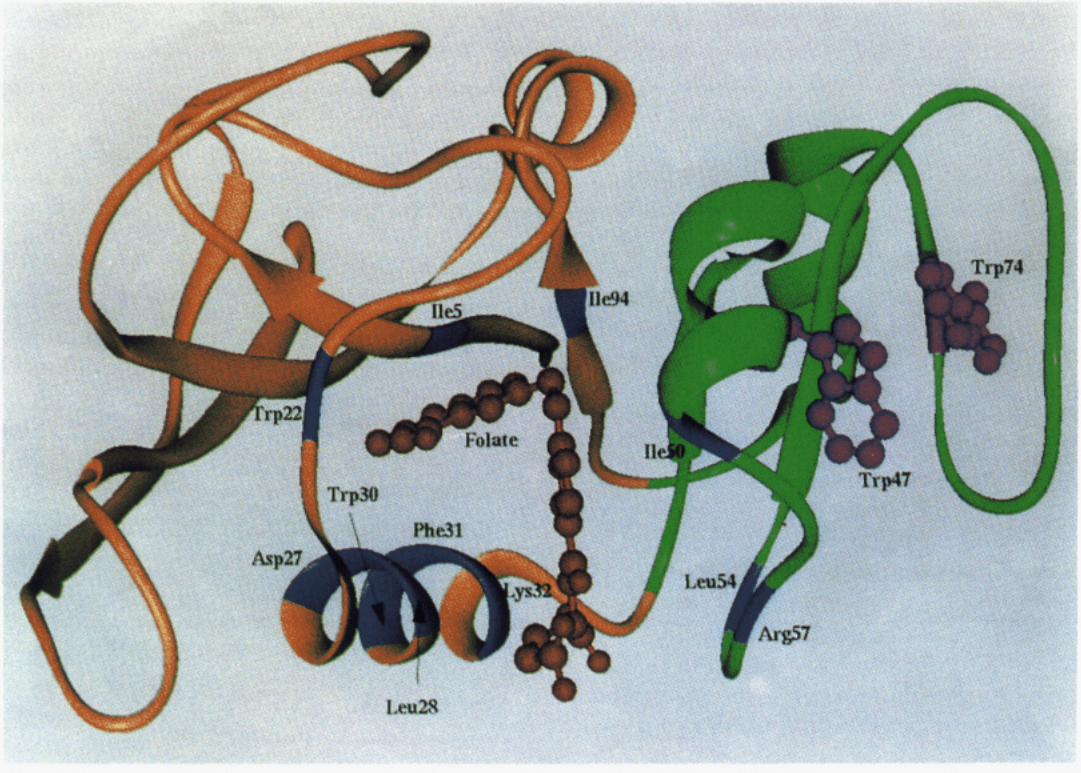

FIGURE 3: Ribbon diagram of DHFR, based upon the X-ray coordinates of the folate–$NADP^+$ ternary complex (Bystroff *et al.*, 1990). Secondary structure elements, folate, and the side chains of Trp47 and Trp74 are also portrayed. The adenine binding domain as defined by Bystroff (strands B, C, and D; Bystroff *et al.*, 1990) is colored green. The backbone locations of residues whose side chains form contacts with folate are indicated in blue.

Table 1: Relaxation Times and Amplitudes for the Refolding of DHFR in 0.6 M Urea at pH 7.80 and 15 °C Observed by Various Methods

	relaxation times (s)				relative amplitudes (%)			
phase	ANS Fl[a]	Trp Fl[b]	SF-CD[c]	MTX[d]	ANS Fl[a]	Trp Fl[b]	SF-CD[c]	MTX[d]
τ_1	125 ± 9	145 ± 9	ND[e]	220 ± 70	4	8	ND[e]	5
τ_2	45 ± 3	52 ± 7	63 ± 9	55 ± 10	27	22	17	13
τ_3	10 ± 2	10.5 ± 3	11.1 ± 0.4	11 ± 1.3	7	8	27	23
τ_4	1.65 ± 0.01	1.3 ± 0.1	0.9 ± 0.1	1.3 ± 0.01	62	62	56	58
τ_5	0.25 ± 0.01	0.26 ± 0.06	0.20 ± 0.03	ND[f]	ND[f]	ND[f]	ND[f]	ND[f]

[a] ANS binding. Errors are the standard deviations from the average of three runs. The amplitudes of each of the phases in terms of photomultiplier tube voltage were +4.4, +2.8, −4.0, −0.45, −1.7, and −0.26 V for the burst phase and the τ_5, τ_4, τ_3, τ_2, and τ_1 phases, respectively. [b] Tryptophan fluorescence experiment data taken from Jennings *et al.* (1993). Errors are standard deviations from the average of three runs. [c] Stopped-flow CD; B. E. Jones and C. R. Matthews, unpublished results. Errors are standard deviations obtained from nonlinear least squares fitting. [d] MTX-binding experimental data taken from Touchette *et al.* (1986). Errors are standard deviations from the average of four runs. [e] Not determined due to low amplitude of the τ_1 phase by this technique (Kuwajima *et al.*, 1991). [f] Not determined. Because the τ_5 phase appears as a lag phase in MTX binding experiments, only the relative amplitudes of the τ_1−τ_4 phases were calculated for direct comparison.

by testing the effect of varying the ANS concentration on the relaxation times. The similarity of the relaxation times observed by ANS fluorescence, tryptophan fluorescence (Jennings *et al.*, 1993), and far-UV CD spectroscopy (Kuwajima *et al.*, 1991; Table 1) demonstrates that ANS binding does not perturb any of the refolding reactions of DHFR. Also, varying the ANS concentration at constant DHFR concentration did not change these relaxation times (data not shown). The amplitudes of all five phases increased in a similar and linear fashion from 10 to 300 μM ANS, implying that the dissociation constant of ANS for these folding intermediates must be greater than 250 μM. This dissociation constant implies that, under the conditions of these experiments (20 μM DHFR and 200 μM ANS), the maximum enhancement of the stability of the folding intermediates by ANS binding must be less than 0.3 kcal mol^{-1}. Although the burst phase species is only marginally stable and could be affected by a contribution of this magnitude from ANS binding, the close parallel in the loss of amplitude of this phase with increasing urea concentration with that from stopped-flow CD studies performed in the absence of ANS [Figure 2 in Kuwajima *et al.* (1991)] demonstrates that the actual perturbation in stability is minimal. The stabilities of the I_1−I_4 intermediates, estimated from the ratios of the rate-limiting unfolding and refolding rates in the absence of denaturant, are approximately 3 kcal mol^{-1} (Jennings and Matthews, unpublished results). Therefore, these species are even less likely to be perturbed by ANS binding. Taken together, these data support the conclusion that the ANS fluorescence technique accurately monitors the folding reaction of DHFR.

Relative Stabilities of Folding Intermediates. The refolding of DHFR in the presence of ANS was carried out at varying final urea concentrations to investigate the stabilities of the different intermediate states. Because the rate of formation of the set of burst phase intermediates, I_{BP_1}−I_{BP_4}, is at least 50 times faster than the next fastest, τ_5, phase, the amplitude of the burst phase can be used as a measure of the populations of these intermediates (Mann & Matthews, 1993; Kuwajima *et al.*, 1987; Ikeguchi *et al.*, 1986). The dependence of the burst phase amplitude in ANS fluorescence on the final urea concentration at 15 °C and pH 7.8 is shown in Figure 4A. The simple, hyperbolic shape of this curve suggests that the burst phase intermediates have marginal stability. The transition curve derived from monitoring the amplitude of the burst phase detected by stopped-flow CD spectroscopy (Kuwajima *et al.*, 1991) has a similar

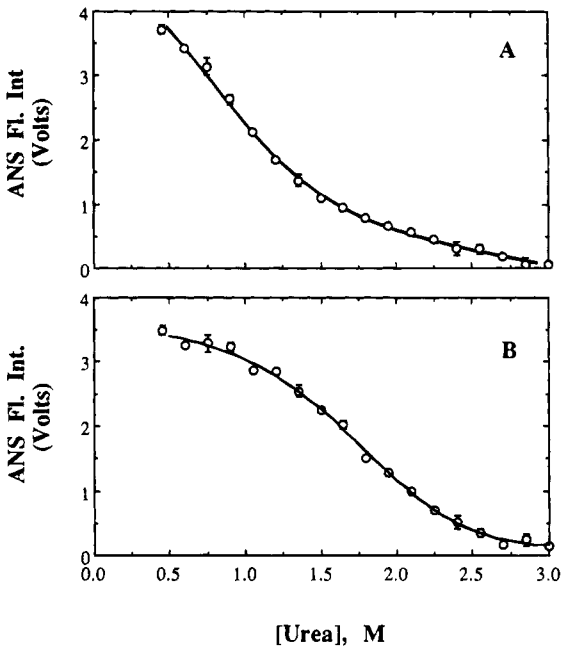

FIGURE 4: Urea titrations of the burst phase (A) and τ_5 (B) amplitudes observed by ANS binding during refolding from 5.4 M urea to the indicated final urea concentration. Amplitudes were taken from the nonlinear least squares fit to a sum of exponentials; error bars (where visible) indicate the standard deviations of three separate jumps. Lines are drawn to aid the eye. Attempts to obtain refolding data at lower final urea concentrations were unsuccessful due to inconsistent mixing at the high dilutions necessary. The final protein and ANS concentrations were 10 and 200 μM, respectively. The buffer was identical to that described in Figure 2.

shape, supporting the conclusion of marginal stability for these intermediates relative to the unfolded form.

The stabilities of the I_1−I_4 intermediates can be qualitatively probed in similar fashion by examining the urea dependence of the amplitude of the τ_5 phase in folding detected by ANS binding (Figure 4B). This transition displays a sigmoidal shape, which is characteristic of cooperatively folded structure. An estimate of the stability from these data is precluded by complications arising from (1) the urea dependence of the preceding intermediates, (2) the subsequent τ_4 phase which conveys 58% of the protein to a native-like conformer but is only a factor of 5 slower than the τ_5 reaction (Table 1), and (3) the fact that the τ_5 phase represents the combined formation of four intermediates (Figure 1). Even with these limitations, these data clearly show that the free energies of folding of the I_1−I_4 species are greater than those of the burst phase intermediates.

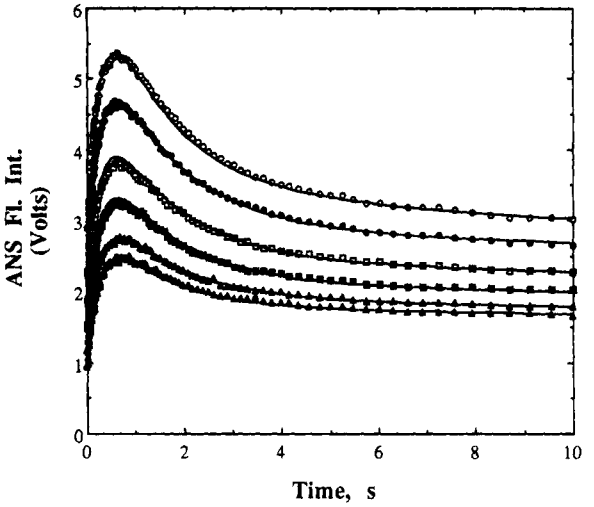

FIGURE 5: Representative ANS traces observed at different acrylamide concentrations for DHFR refolding jumps from 5.4 M urea to 0.6 M urea. Concentrations of acrylamide were 0.0 M (open circles), 0.1 M (filled circles), 0.2 M (open squares), 0.3 M (filled squares), 0.4 M (open triangles), and 0.5 M (filled triangles). Lines through the data are fits using eq 1. The final protein concentration was 20 μM, and the final ANS concentration was 200 μM in all experiments. The buffer was identical to that described in Figure 2.

Fluorescence Quenching Studies. The further increase in ANS fluorescence intensity in the τ_5 phase could have two explanations: (1) it reflects the formation of additional binding sites which are similar to those formed in the burst phase or (2) it reflects the formation of a different class of binding sites in which the dye is more sequestered from solvent and, therefore, fluoresces with greater intensity. To differentiate between the possibilities, polar quenching agents were included in the refolding mixture along with ANS. If ANS becomes more excluded from solvent in the τ_5 phase, then it ought to be less susceptible to water-soluble quenching agents than in the burst phase.

A series of ANS fluorescence traces obtained at increasing acrylamide concentration are shown in Figure 5. When these data were fit to a sum of five exponentials, the amplitudes of each fitted phase and the burst phase were found to decrease monotonically with increasing quencher concentration (data not shown). Qualitatively similar results were obtained using the cationic Cs^+ and anionic I^- agents (data not shown). For the charged quenching agents, the ionic strength of the solution was maintained at 0.5 M by the addition of KCl. The intensities of free ANS were not observed to vary significantly under any of the solvent conditions, presumably because of its low quantum yield (Turner & Brand, 1968) and its short emission lifetime in aqueous solution (J. Beechem, personal communication).

The solvent accessibility of the ANS bound to the folding intermediates of DHFR can be determined from these data by calculating the fluorescence intensities of each species as a function of quencher concentration. The observed molar fluorescence intensity at any time during the refolding reaction, $\mathbf{F}_{tot}(t)$, is the sum of the fluorescence intensity of each species, F_i, weighted by its relative concentration, $C_i(t)/C_{tot}$. $C_i(t)$ is the time-dependent concentration specified by the folding mechanism. This situation can be represented mathematically as

$$\mathbf{F}_{tot}(t) = \sum[F_i(C_i(t)/C_{tot})] \quad (1)$$

The kinetic folding mechanism of DHFR (Figure 1) is proposed to follow a combination of sequential and parallel reactions, involving a common unfolded form, U, a set of burst phase intermediates, $I_{BP_1}-I_{BP_4}$, a set of four intermediates which are formed in the τ_5 phase, I_1-I_4, and a set of four native conformers, N_1-N_4, which form via parallel channels in the $\tau_1-\tau_4$ reactions (Jennings *et al.*, 1993). The assumption that the burst phase reaction leads to a set of intermediates, $I_{BP_1}-I_{BP_4}$, is supported by results from pulse-labeling NMR experiments which indicate that at least two distinct populations exist after 6 ms (Jones and Matthews, submitted). Assuming that the burst phase reaction is essentially complete before the subsequent folding reactions begin and that interconversions between channels are slower than folding through each channel, the mechanism for each channel can be represented by a simple, three-state model:

$$I_{BP_i} \xrightarrow{k_f} I_i \xrightarrow{k_{si}} N_i \quad (2)$$

where I_{BP_i} represents the burst phase intermediate which will flow through channel i, I_i is the intermediate formed in the τ_5 reaction (i.e., I_1-I_4), and N_i is the native conformer for that particular channel. k_f is assumed to be the same for each of the channels; however, k_{si} is allowed to vary, reflecting the four phases, $\tau_1-\tau_4$, which lead to the set of native conformers. This model also presumes that, because the experiments are done under strongly refolding conditions, the reverse reactions for these steps are absent. This assumption seems reasonable because I_i and N_i are fully folded at 0.6 M urea (Figure 4 and Touchette *et al.*, 1986).

The time-dependent concentrations of these species, $C_i(t)$, can be expressed in terms of the microscopic rate constants, k_f and k_{si}, and the initial concentration of unfolded protein flowing through each channel, $[I_{BP(0)}]_i$ (Fersht, 1985):

$$[I_{BP}(t)_i] = [I_{BP(0)}]_i \exp(-k_f t) \quad (3a)$$

$$[I_i(t)] = [I_{BP(0)}]_i(k_{si} - k_f)^{-1} \times k_f [\exp(-k_f t) - \exp(-k_{si} t)] \quad (3b)$$

$$[N_i(t)] = [I_{BP(0)}]_i\{1 + (k_f - k_{si})^{-1} \times [k_{si} \exp(-k_f t) - k_f \exp(-k_{si} t)]\} \quad (3c)$$

The amount of protein flowing through each channel, $[I_{BP(0)}]_i$, was calculated from the total concentration of protein and the fraction of MTX which binds in that phase. In the standard buffer, the τ_1, τ_2, τ_3, and τ_4 channels bind 6%, 13%, 23%, and 58%, respectively, of a stoichiometric amount of MTX present during folding (Table 1; Touchette *et al.*, 1986; Jennings *et al.*, 1993). In the presence of 0.5 M salt, these proportions change to 5%, 13%, 12%, and 70%, respectively.

Several additional assumptions had to be made to achieve convergent fits of the ANS fluorescence traces to these equations. The fluorescence intensity of the dye bound to each of the native conformers was assumed to be identical. This assumption seems reasonable given the existence of a single, tight-binding MTX site in each conformer and the propensity of ANS to bind to this site. The intensity of ANS bound to individual populations of the burst phase intermediates was assumed to be identical, in the absence of data to the contrary. Note that the marginal stability of these

intermediates (Figure 4) means that, immediately after folding begins, the protein will be distributed between the unfolded form and the burst phase intermediates. As a result, the ANS signal will be reduced by the fraction which remains unfolded after 5 ms. This reduction in signal will yield a lower apparent fluorescence intensity for these intermediates but will have no effect on the Stern–Volmer or static quenching constants (see below). It was also necessary to specify the rate constant for the slowest folding phase, i.e., the τ_1 channel. Under strongly folding conditions, this rate constant is expected to be the reciprocal of the observed relaxation time (Table 1; Bernasconi, 1976; Matthews, 1987). The small amplitude and long relaxation time make the computer fit of this phase less precise than its faster counterparts.

The data for the ANS fluorescence intensity, $\mathbf{F}_{tot}(t)$, were then fit to eq 1 using a nonlinear least squares fitting program; the excellent quality of the fits is shown in Figure 5. The ANS fluorescence intensities of burst phase species, the I_1–I_4 intermediates, and the native conformation were all found to decrease in a progressive fashion as the concentrations of all three quenching agents were increased (data not shown). The rate constants for the τ_2, τ_3, τ_4, and τ_5 phases obtained (data not shown) were within 10% of the relaxation times obtained from the direct fit of the ANS fluorescence data to five exponentials ($k = \tau^{-1}$; Table 1). The agreement supports the simplifications in the folding model required to fit the quenching data.

The fluorescence intensity data were combined with the intensities in the absence of quencher and plotted in the typical Stern–Volmer fashion, i.e., as plots of F_0/F vs [quencher], where F and F_0 are the fluorescence intensities in the presence and absence of quencher, respectively (Lakowicz, 1986). The results with the exception of the I_1 intermediate are shown in Figure 6. The small magnitude of the τ_1 phase precluded accurate measurements of the fluorescence intensity for the associated I_1 intermediates. These plots display upward curvature at increasing quencher concentration for the set of burst phase intermediates (I_{BP}), the I_4, and the I_3 species but a linear dependence for the native and the I_2 species. A linear dependence in Stern–Volmer plots indicates the dominance of dynamic quenching, while nonlinear behavior suggests that there are significant contributions from both dynamic and static quenching (Lakowicz, 1986). An expression containing terms representing both mechanisms is required to obtain an accurate description of these data (Eftink & Ghiron, 1981; Birks, 1970):

$$F_0/F = (1 + K_{SV}[Q])e^{V[Q]} \quad (4)$$

where [Q] is the quencher concentration, K_{SV} is the Stern–Volmer constant for the dynamic quenching process, and V is the static quenching constant. The values of K_{SV} and V for each species in the presence of acrylamide, Cs^+, and I^- are shown in Table 2. As a check on the validity of the values calculated for the native conformation, dynamic and static quenching constants for ANS bound to DHFR in its native form were obtained for all three quenchers by equilibrium methods; these values are also shown in Table 2. The excellent agreement between the quenching constants for the native conformation obtained from kinetic and equilibrium methods also supports the fit of the kinetic data to the above model.

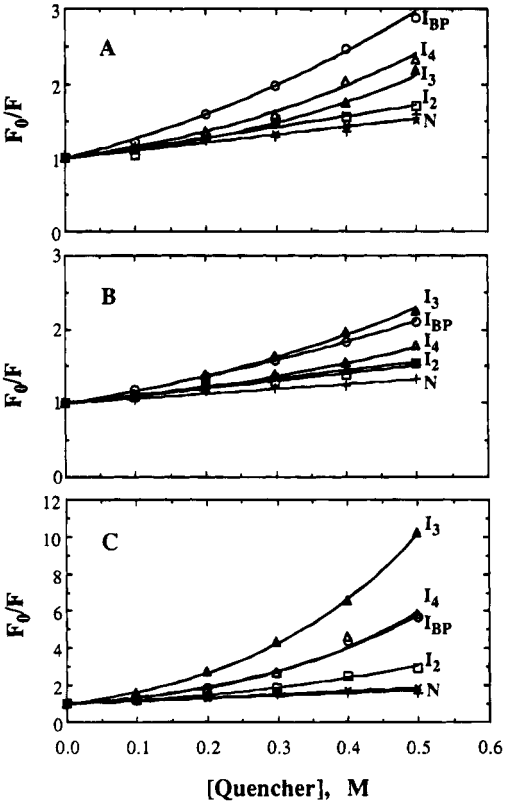

FIGURE 6: Stern–Volmer plots for the various folding intermediates in the presence of acrylamide (A), Cs^+ (B), and I^- (C). Symbols plotted are burst phase intermediates (I_{BP}; open circles), I_2 (open squares), I_3 (filled triangles), I_4 (open triangles), native from kinetic data (×), and native from equilibrium data (+). Data plotted were the averages of results from fits to three individual runs at each quencher concentration. The refolding jumps were from 5.4 M urea to 0.6 M urea, with a final protein concentration of 20 μM and an ANS concentration of 200 μM. For experiments using either I^- or Cs^+, the total salt concentration was maintained at 0.5 M by the addition of KCl.

In the presence of acrylamide, the common K_{SV} value for the burst phase intermediates (I_{BP}) is significantly larger than that for any of the other intermediates or the native conformation. This result demonstrates that ANS is relatively exposed to solvent when bound to I_{BP}, at least in comparison to the other conformers. Note that because the observed fluorescence intensity, F, is normalized against the intensity in the absence of quencher, F_0, the values of K_{SV} and V for the burst phase intermediates are not affected by the partial shift of the unfolded protein to these marginally stable species. The K_{SV} values of the remaining species, including the native conformation, are smaller and almost within experimental error, arguing for similar, more solvent-excluded environments for ANS. Because the static quenching constants for I_2 and N are essentially zero, it appears that acrylamide cannot bind in the vicinity of the ANS in these conformers. The similar behavior of I_2 and N may reflect the fact that I_2 is the only intermediate which folds to a native conformer (N_2) that can bind both MTX and $NADP^+$ (Jennings *et al.*, 1993; Jones, Jennings and Matthews, unpublished results). Nonzero V values for I_{BP}, I_3, and I_4 suggest that acrylamide binds to these species in the vicinity of the ANS and induces static quenching.

The variation in the Stern–Volmer constants for dynamic quenching by Cs^+ is very similar to that observed for the neutral acrylamide. The set of I_{BP} species again has the highest value for K_{SV}, although the K_{SV} for I_3 is within

Table 2: Stern–Volmer Constants (K_{SV}) and Static Quenching Constants (V) for ANS Bound to the Folding Intermediates of DHFR at 15 °C

	quencher					
	acrylamide		Cs^+		I^-	
species	$K_{SV}(M^{-1})$	$V(M^{-1})$	$K_{SV}(M^{-1})$	$V(M^{-1})$	$K_{SV}(M^{-1})$	$V(M^{-1})$
I_{BP}	2.5 ± 0.1[a]	0.9 ± 0.2	1.60 ± 0.03	0.67 ± 0.04	2.9 ± 0.4	2.4 ± 0.3
I_2	1.4 ± 0.1	0.06 ± 0.04	1.0 ± 0.2	0.06 ± 0.04	1.8 ± 0.3	1.7 ± 0.4
I_3	1.0 ± 0.1	1.6 ± 0.2	1.5 ± 0.2	1.1 ± 0.3	5.0 ± 0.2	2.6 ± 0.1
I_4	1.4 ± 0.2	1.4 ± 0.3	0.84 ± 0.07	1.2 ± 0.2	2.6 ± 0.5	2.7 ± 0.5
N (kin)[b]	1.08 ± 0.04	0.02 ± 0.1	1.1 ± 0.1	0.01 ± 0.3	1.8 ± 0.1	0.06 ± 0.05
N (eq)[c]	1.09 ± 0.08	0.01 ± 0.2	0.8 ± 0.1	0.03 ± 0.04	1.6 ± 0.1	0.05 ± 0.04

[a] Errors are the standard deviations from the nonlinear least squares fits of the F_0/F values to eq 4. [b] Obtained from fits of the kinetic data as described in the text. [c] Obtained from titrations of ANS bound to native DHFR at equilibrium.

experimental error. The K_{SV} values for the remaining intermediates and the native form are essentially equal and of similar magnitude, indicating a greater degree of protection from solvent. The static quenching constants show precisely the same trend as for acrylamide, demonstrating that static mechanisms for these neutral and cationic quenchers are only significant for the I_{BP}, I_3, and I_4 species.

The results obtained with I^- (Table 2) compare reasonably well with those for acrylamide or Cs^+. The notable differences are the large K_{SV} value for I_3 and the occurrence of static quenching for all but the native conformation. The negative charge on iodide may influence its ability to induce static and dynamic quenching in the various folding intermediates for DHFR.

DISCUSSION

ANS has proven to be a sensitive probe for monitoring the folding of globular proteins, including, as is shown in this paper, dihydrofolate reductase. For carbonic anhydrase, α-lactalbumin (Semisotnov *et al.*, 1991), and DHFR, the fluorescence intensity of ANS increases dramatically within the dead time of mixing of stopped-flow instruments (<20 ms, Semisotnov *et al.*, 1991; <5 ms, these results). For all three proteins, this burst phase reaction is followed first by a further increase in intensity over the next few hundred milliseconds and then a subsequent decrease as the protein folds to the native conformation. The similar response of three different proteins suggests that the development of nonpolar surfaces during folding may follow a common pathway.

Formation of Nonpolar Surfaces during the Folding of DHFR. A part of the interpretation of these results requires insight into the nature of the ANS binding sites on these early folding intermediates. As was shown in the present study on DHFR, the fluorescence intensity of ANS bound to the set of burst phase intermediates is significantly more sensitive to dynamic quenching by acrylamide than for the subsequent set of I_1–I_4 intermediates. Cs^+ gives very similar results with the exception that the quenching of the I_3 intermediate is as effective as for I_{BP}; electrostatic interactions between Cs^+ and either the protein or the anionic sulfonate group on ANS or both may account for the differential response of I_3. These results demonstrate that the enhanced intensity in the few hundred millisecond time range reflects the formation of a new class of ANS binding sites which are, in general, less accessible to water-soluble quenching agents rather than to the formation of additional binding sites of the sort presented by the burst phase species. The potential complexities introduced by the presence of formal charges on Cs^+ and I^- suggest that neutral agents such as acrylamide may be more useful in assessing the solvent exposure of ANS bound to proteins.

Semisotnov and his colleagues (Semisotnov *et al.*, 1991) have interpreted the biphasic increase in ANS fluorescence intensity in terms of the sequential formation of a pair of transient intermediates: a premolten globule state and the molten globule state. The premolten globule state is proposed to contain secondary structure and sufficient nonpolar surface to bind ANS but to be more expanded than the molten globule state. The molten globule state has a high content of secondary structure, a compactness of only 10–15% less than that of the native form, and little or no defined tertiary structure (Ptitsyn, 1987; Kuwajima, 1989). Uversky and Ptitsyn (1994) have recently reported an equilibrium intermediate in the unfolding of β-lactamase at low temperature which is less compact than the molten globule state but more compact than the unfolded state. This species could conceivably represent an equilibrium form of the premolten globule state of β-lactamase. In terms of this interpretation, the increase in ANS fluorescence intensity in the hundreds of millisecond time range (Ptitsyn *et al.*, 1990) would reflect the enhanced protection of the dye against solvent-quenching mechanisms by the more compact, molten globule species.

Another possible interpretation of the biphasic increase in ANS fluorescence intensity during folding is that the burst phase reflects binding of the dye to the molten globule species and the subsequent rise in intensity reflects the binding to an intermediate(s) which has folded subdomains and defined tertiary structure. In this case, the enhanced intensity in the hundreds of milliseconds time range might reflect the binding of the dye to solvent-inaccessible sites between folded subdomains. For DHFR, this possibility is consistent with the observation that the protection of ANS from dynamic quenching by acrylamide offered by the set of I_2–I_4 intermediates (and, presumably, I_1) is comparable to that of the native conformation (Table 2). As noted above, ANS binds in the same site as MTX, in the cleft between the two structural domains found in the native conformation (Bystroff *et al.*, 1990).

The results of a previous study of the folding of DHFR using stopped-flow far-UV CD spectroscopy (Kuwajima *et al.*, 1991) show that the later interpretation is correct, at least for DHFR. Examination of the wavelength dependence of the far-UV CD kinetic phase, which corresponds to the τ_5 ANS phase, revealed that it reflects the formation of an exciton between Trp47 and Trp74. The side chains of these residues are part of a hydrophobic core which helps to define

the adenine binding domain in DHFR (Figure 3). The electronic coupling between the chromophores in an exciton pair is sensitive to both the distance and orientation between the transition dipole moments (Cantor & Schimmel, 1980). The close agreement between the amplitudes for the CD τ_5 phase for the wild-type protein and the far-UV CD difference spectrum between the native conformations of wild-type DHFR and the Trp74 → Leu mutant shows that these two tryptophan residues achieve a native-like packing in the hundreds of millisecond time range (Kuwajima *et al.*, 1991). Because this is precisely the same event that the ANS senses as its fluorescence intensity increases to a maximum for DHFR, it is clear that the second stage of ANS intensity increase occurs concomitantly with the development of specific tertiary structure. According to the above definition, this observation rules out the molten globule explanation for this species, at least for DHFR.

Relationship to the Development of Secondary Structure. Comparison of the results of a previous stopped-flow far-UV CD study of the formation of secondary and tertiary structure in DHFR (Kuwajima *et al.*, 1991) with the results of the ANS experiments on the formation of nonpolar surfaces provides insight into the development of higher order structure during folding. The set of I_{BP_i} intermediates, which are formed in <5 ms, has substantial secondary structure *and* nonpolar surface(s). This species has marginal stability relative to the unfolded form, as judged by the gradual loss in amplitude of both the far-UV ellipticity and the ANS fluorescence signals at increasing urea concentration.

The inherent limitations of stopped-flow drive trains and turbulent mixing make it impossible to determine whether the secondary structure precedes the nonpolar surfaces in the I_{BP_i} intermediates, whether the nonpolar surface precedes the secondary structure, or whether both form in a concerted fashion. The submicrosecond time range for the helix/coil transition (Zana, 1975; Cummings & Eyring, 1975) and the observation of helix formation in peptides (Marqusee *et al.*, 1989) are consistent with a model in which elements of secondary structure form first and direct the folding through diffusional/collisional processes (Karplus & Weaver, 1976; Kim & Baldwin 1990; Karplus & Weaver, 1994).

Recently, however, reports of residual structure in the 434 repressor (Neri *et al.*, 1992), the α-subunit of tryptophan synthase (Saab-Rincon *et al.*, 1993), and β-lactamase (Uversky & Ptitsyn, 1994) in high denaturant concentrations suggest that the association of nonpolar side chains may be an important early event in folding. It has also been proposed that a hydrophobic collapse to a compact form may quite naturally give rise to secondary structure because ordered structures are easier to organize in compact forms (Chan & Dill, 1990; Covell & Jernigan, 1990). In the absence of information on folding events in the submillisecond time range, it is impossible to choose between these models. The development of technology to investigate folding reactions which occur between nanoseconds and milliseconds is required; photoinitiated folding reactions may provide a means to obtain such data (Jones *et al.*, 1993).

Following the burst phase reaction, the DHFR folding reaction which occurs in the hundreds of millisecond time range can be detected by tryptophan fluorescence (Touchette *et al.*, 1986), far-UV CD, and ANS fluorescence. The increase in the tryptophan fluorescence was uniquely assigned to Trp74 using mutagenic techniques (Garvey *et al.*, 1989). Mutagenesis also proved that the far-UV CD signal in the same time range reflected the formation of an exciton between Trp47 and Trp74, not changes in the secondary structure (Kuwajima *et al.*, 1991). The development of nonpolar surfaces demonstrated by ANS fluorescence is, therefore, accompanied by the formation of a specific tertiary contact but not by any significant changes in secondary structure. The driving force for this reaction must derive from the establishment of more favorable van der Waals interactions between side chains, not from changes in backbone hydrogen-bonding patterns. Udgaonkar and Baldwin (1990) have reported that a burst phase set of amide protons in ribonuclease A experience increased protection from exchange with solvent in the several hundred millisecond time range. The lack of protection for additional amide protons in this same transition suggests that enhanced van der Waals interactions are again the driving force for this folding reaction. Perhaps these enhanced packing interactions resemble the solid-like interior of fully folded proteins (Richards, 1977).

The final, rate-limiting steps in the folding of DHFR involve further changes in the secondary structure (Kuwajima *et al.*, 1991), the further packing of tryptophan residues in hydrophobic pockets (Jones, Beechem, and Matthews, submitted), and a decrease in the exposure of nonpolar surfaces to solvent. MTX binding sites appear in all four native conformers, but the $NADP^+$ site only arises in the N_2 conformer (Jennings *et al.*, 1990). Mutational analysis has also shown that a variety of polar and nonpolar side chains alter their interactions with their environments as the native conformers appear (Perry *et al.*, 1987; Garvey & Matthews, 1989). Taken together, these results demonstrate that the formation of cooperatively folded native conformation occurs with global changes in all types of noncovalent interactions.

General Implications. These results suggest that the folding of DHFR involves three distinct stages: (1) the rapid (<5 ms) formation of a set of intermediates which contain secondary structure and exposed hydrophobic surfaces, (2) further folding to a set of intermediates which contain subdomains of tertiary structure, and (3) the rate-limiting formation of native conformers. Recent studies with hen lysozyme suggest that such a scheme may be a general description of events that occur during the folding of proteins. Dobson and co-workers (Itzhaki *et al.*, 1994) demonstrated that the solvent accessibility of tryptophans reaches a native-like level after the formation of secondary structure but prior to the development of the active site during refolding. These authors suggested that the rate-limiting steps involve a docking of two domains containing native-like secondary structure to form the active site.

The common response of ANS fluorescence during the folding of DHFR, carbonic anhydrase, and α-lactalbumin suggests that the development of nonpolar surfaces in all three proteins follows a similar progression of events. A more limited study on the folding of β-lactamase, phosphoglycerate kinase, and β-lactoglobulin by Ptitsyn *et al.* (1990) also demonstrated kinetic phases where the ANS fluorescence intensity increases before subsequent decreases to the intensity found for the native form. Whether these phases correspond to burying ANS in nonpolar pockets which are defined by specific tertiary structure, as is seen for DHFR, or whether they reflect binding to molten globules remains

to be tested. Comparison of such results with those from far-UV CD experiments would elucidate the temporal formation of secondary structure and nonpolar surface protein folding and, potentially, the roles of the hydrophobic effect and hydrogen bonding at various stages in this complex process.

ACKNOWLEDGMENT

We thank Dr. W. D. Horrocks, Jr., for use of his Spex Fluorolog spectrometer and Luis Reynaldo for assistance in acquiring and analyzing the data. We also thank Drs. Craig Mann and Colin Gegg for critical reviews of the manuscript and Dr. Joseph Beechem and Micheal Otto for helpful comments and discussion.

REFERENCES

Bernasconi, C. F. (1976) *Relaxation Kinetics*, pp 20−38, Academic Press, New York.
Birks, J. B. (1970) *Photophysics of Aromatic Molecules*, pp 433−447, Wiley-Interscience, New York.
Briggs, M. S., & Roder, H. (1992) *Proc. Natl. Acad. Sci. U.S.A. 89*, 2017−2021.
Bystroff, C., Oatley, S. J., & Kraut, J. (1990) *Biochemistry 29*, 3263−3277.
Cantor, C. R., & Schimmel, P. R. (1980) *Biophysical Chemistry*, W. H. Freeman and Co., New York.
Chan, H. S., & Dill, K. A. (1990) *Proc. Natl. Acad. Sci. U.S.A. 87*, 6388−6392.
Chen, Y. W., Fersht, A. R., & Henrick, K. (1992) *J. Mol. Biol. 234*, 1158−1170.
Covell, D. G., & Jernigan, R. L. (1990) *Biochemistry 29*, 3287−3294.
Cummings, A. L., & Eyring, E. M. (1975) *Biopolymers 14*, 2107−2114.
Dao-pin, S., Anderson, D. E., Baase, W. A., Dahlquist, F. W., & Matthews, B. W. (1991) *Biochemistry 30*, 11521−11529.
Dill, K. A. (1990) *Biochemistry 29*, 7133−7155.
Eftink, M. R., & Ghiron, C. A. (1981) *Anal. Biochem. 114*, 672−680.
Fersht, A. (1985) *Enzyme Structure and Mechanism*, pp 121−154, W. H. Freeman & Co., New York.
Frieden, C. (1990) *Proc. Natl. Acad. Sci. U.S.A. 87*, 4413−4416.
Garvey, E. P., & Matthews, C. R. (1989) *Biochemistry 28*, 2083−2093.
Garvey, E. P., Swank, J., & Matthews, C. R. (1989) *Proteins: Struct., Funct., Genet. 6*, 259−266.
Goldenberg, D. P., Frieden, R. W., Haack, J. A., & Morrison, T. B. (1989) *Nature 338*, 127−132.
Hillcoat, B. L., Nixon, P. F., & Blakely, R. L. (1967) *Anal. Biochem. 21*, 178.
Ikeguchi, M., Kuwajima, K., Mitani, M., & Sugai, S. (1986) *Biochemistry 25*, 6965−6972.
Itzhaki, L. S., Evans, P. A., Dobson, C. M., & Radford, S. E. (1994) *Biochemistry 33*, 5215−5220.
Jennings, P. A., & Wright, P. E. (1993) *Science 262*, 892−896.
Jennings, P. A., Finn, B. E., Jones, B. E., & Matthews, C. R. (1993) *Biochemistry 32*, 3783−3789.
Jones, C. M., Henry, E. R., Hu, Y., Chan, C., Luck, S. D., Bhuyan, A., Roder, H., Hofrichter, J., & Eaton, W. A. (1993) *Proc. Natl. Acad. Sci. U.S.A. 90*, 11860−11864.
Karplus, M., & Weaver, D. L. (1976) *Nature 260*, 404−406.
Karplus, M., & Weaver, D. L. (1994) *Protein Sci. 3*, 650−668.
Kauzmann, W. (1959) *Adv. Protein Chem. 14*, 1−63.
Kim, P. S., & Baldwin, R. L. (1990) *Annu. Rev. Biochem. 59*, 631−660.
Kuwajima, K. (1989) *Proteins 6*, 87−103.
Kuwajima, K., Yamaya, H., Miwa, S., Sugai, S., & Nagamura, T. (1987) *FEBS Lett. 221*, 115−118.
Kuwajima, K., Garvey, E. P., Finn, B. E., Matthews, C. R., & Sugai, S. (1991) *Biochemistry 30*, 7693−7703.
Laemmli, U. K. (1970) *Nature 227*, 680−685.
Lakowicz, J. R. (1986) *Principles of Fluorescence Spectroscopy*, pp 258−295, Plenum Press, New York.
Loewenthal, R., Sancho, J., Reinikainen, T., & Fersht, A. R. (1992) *J. Mol. Biol. 232*, 574−583.
Mann, C. J., & Matthews, C. R. (1993) *Biochemistry 32*, 5282−5290.
Marqusee, S., Robbins, V. H., & Baldwin, R. L. (1989) *Proc. Natl. Acad. Sci. U.S.A. 86*, 5286−5290.
Matouschek, A., Kellis, J. T., Jr., Serrano, L., & Fersht, A. R. (1989) *Nature 340*, 122−126.
Matouschek, A., Serrano, L., & Fersht, A. R. (1992) *J. Mol. Biol. 224*, 819−835.
Matthews, C. R. (1987) *Methods Enzymol. 154*, 498−511.
Neri, D., Billeter, M., Wider, G., & Wüthrich, K. (1992) *Science 257*, 1559−1563.
Pace, C. N. (1975) *Crit. Rev. Biochem. 3*, 1−43.
Perry, K. M., Onuffer, J. J., Gittelman, M. S., Barmat, L., & Matthews, C. R. (1989) *Biochemistry 28*, 7961−7968.
Peterman, B. F. (1979) *Anal. Biochem. 93*, 442−444.
Ptitsyn, O. B. (1987) *J. Protein Chem. 6*, 273−293.
Ptitsyn, O. B., Pain, R. H., Semisotnov, G. V., Zerovnik, E., & Razgulyaev, O. I. (1990) *FEBS Lett. 262*, 20−24.
Richards, F. M. (1977) *Annu. Rev. Biophys. Bioeng. 6*, 151−176.
Saab-Rincon, G., Froebe, C. L., & Matthews, C. R. (1993) *Biochemistry 32*, 13981−13990.
Semisotnov, G. V., Rodionova, N. A., Razgulyaev, O. I., Uversky, V. N., Gripas, A. F., & Gilmanshin, R. I. (1991) *Biopolymers 31*, 119−128.
Serrano, L., Kellis, J. T., Jr., Cann, P., Matouschek, A., & Fersht, A. R. (1992) *J. Mol. Biol. 224*, 783−804.
Shirley, B. A., Stanssens, P., Hahn, U., & Pace, C. N. (1992) *Biochemistry 31*, 725−732.
Stone, S. R., Montgomery, J. A., & Morrison, J. F. (1984) *Biochem. Pharmacol. 29*, 5195−5202.
Stryer, L. (1965) *J. Mol. Biol. 13*, 482−495.
Tonomura, B., Nakatani, H., Ohnishi, M., Yamaguchi-Ito, J., & Hiromi, K. (1978) *Anal. Biochem. 84*, 370−383.
Touchette, N. A., Perry, K. M., & Matthews, C. R. (1986) *Biochemistry 25*, 5445−5452.
Turner, D. C., & Brand, L. (1968) *Biochemistry 7*, 3381−3390.
Udgaonkar, J. B., & Baldwin, R. L. (1990) *Proc. Natl. Acad. Sci. U.S.A. 87*, 8197−8201.
Uversky, V. N., & Ptitsyn, O. B. (1994) *Biochemistry 33*, 2782−2791.
Zana, R. (1975) *Biopolymers 14*, 2425−2428.